International Journal of Engineering and Advanced Technology (IJEAT)
ISSN: 2249-8958 (Online), Volume-1 Issue-6, August 2012

Natural Convection Heat Transfer of Nanofluids Due to Thermophoresis and Brownian Diffusion in a Square enclosure

Aminreza Noghrehabadi, Amin Samimi

Abstract*— This paper reports a numerical study on natural convection heat transfer and fluid flow in a square cavity filled with CuO–Water nanofluids. Both upper and lower surfaces are being insulated, whilst a uniform constant temperature field applied in horizontal walls. The governing equations of fluid flow are discretized using a finite volume method with a collocated grid arrangement. The numerical results are reported for the effect of Rayleigh number, solid volume fraction and both presence and absence of thermophoresis and Brownian motion effects. The numerical results show that an improvement in heat transfer rate was registered for the whole range of Rayleigh numbers when Brownian and thermophoresis effects are considered.

***Index Terms*— Natural convection; nanofluid; thermophoresis; Brownian motion; cavity**

I. INTRODUCTION

Natural convection heat transfer in enclosures is an important phenomenon in engineering systems due to its wide applications in building heating, automotive technology, solar technology cooling of electronic equipment, etc [1–3]. Improvement in the heat transfer performance of these systems is an essential topic from an energy saving perspective. With this aim, an innovative technique to enhance heat transfer rate by using nanoscale particles (smaller than 100 nm) suspended in the base fluid, has emerged. Engineered suspensions of nanoparticles in liquids, known recently as nanofluid, have generated considerable interest for their potentials to enhance the heat transfer rate in engineering systems. Nanofluids are made from various materials, such as oxide ceramics (Al_2O_3, CuO), nitride ceramics (AlN, SiN), carbide ceramics (SiC, TiC), metals (Cu, Ag, Au), semiconductors, (TiO_2, SiC), carbon nanotubes, and composite materials such as alloyed nanoparticles or nanoparticle core–polymer shell composites [4]. The base media of nanofluids are usually water, oil, acetone, decene, ethyleneglycol, etc. Compared with conventional heat transfer such as oil, water and ethylene glycol mixture, nanofluids have significantly higher thermal conductivity that consequently enhances the heat transfer characteristics of these fluids.

Manuscript published on 30 August 2012.
***** Correspondence Author (s)
Aminreza Noghrehabadi Department of Mechanical Engineering, Shahid Chamran University of Ahvaz, Ahvaz, Iran.
Amin Samimi, Department of Mechanical Engineering, Shahid Chamran University of Ahvaz, Ahvaz, Iran.

Natural convection heat transfer of nanofluid has drawn attraction of many researchers in recent years. It was for the first time Khanaferet et al. [5] who studied natural convection of Cu–water nanofluids in a two-dimensional rectangular enclosure. These authors reported that increasing the buoyancy parameter and volume fraction causes an increase in the average heat transfer coefficient at any given Grashof number. Influences of nanoparticles on the natural convection heat transfer enhancement in horizontal annuli with nanofluids containing various nanoparticles been analyzed numerically by Abu–Nada et al. [6]. They reported an enhancement of heat transfer in horizontal annuli. Shahi et al. [7] investigated the effect of Rayleigh number, solid concentration and heat source location on entropy generation due to natural convection of a nanofluid in a cavity with a protruded heat source.

Natural convection in square cavity with two pairs of heat source–sink filled with water–CuO nanofluid numerically performed by Aminossadati and Ghasemi [8]. They concluded that the rate of heat transfer increases with an increase of the Rayleigh number and the solid volume fraction in both cases of the position of the pairs of source–sink. Yu et al. [9] investigated transient natural convection heat transfer of aqueous nanofluids in a differentially heated square cavity. They concluded that the time–averaged Nusselt number is lowered with increasing volume fraction of nanoparticles at constant Rayleigh numbers. Furthermore, various aspects of the problem have been investigated by Lai and Yang [10], Oztop and Abu–Nada [11], Abunada and Masoud [12], etc [13-23]. The most recently, Oztab et al. [24] investigated the effect of both thermophoresis and Brownian motion on natural convection of Cuo–Water nanofluid for Rayleigh–Bénard problem. They observed that higher heat transfer is formed when Brownian and thermophoresis effects are considered.

In the present study the effect of thermophoresis and Brownian motion on natural convection of Cuo–Water nanofluid in square cavity has been investigated numerically. To the best knowledge of the authors, no study which considers this problem has yet been reported in the literature. As such, the focus of this paper is to examine the effects of pertinent parameters such as Rayleigh number, solid volume fraction, thermophoresis and Brownian motion on the nanoparticles distribution and natural convection characteristics of a square enclosure filled with a nanofluid.

II. PHYSICAL MODEL

The physical model under consideration is natural convection in a square enclosure of side length L schematically shown in Fig. 1.

The left vertical wall is maintained at a constant temperature t_h higher than the constant temperature t_c of the of the right vertical wall. Other walls of the enclosures are all thermally insulated.

The fluid in the enclosure is a water based nanofluid containing CuO nanoparticles. The nanofluid is assumed incompressible and Newtonian and only Brownian diffusion and thermophoresis are important slip mechanisms between the two media. Water and CuO nanoparticles are in thermal equilibrium and the flow is also conceived as laminar and two-dimensional.

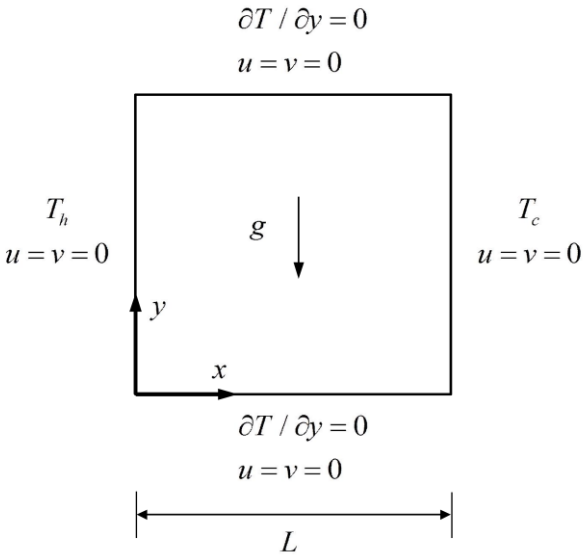

Fig. 1. A schematic diagram for the problem with boundary conditions.

The thermophysical properties of the nanofluid are listed in Table 1. The density of the nanofluid is approximated by the standard Boussinesq model. The viscosity and the thermal conductivity of the nanofluid are considered as variable properties; both vary with temperature and volume fraction of nanoparticles.

TABLE I. Termophisical Progrid Independence Study

Physical properties	**Fluid phase (water)**	**CuO**
C_p (J/kg K)	4179	540
ρ (kg/m3)	997.1	6500
k (W/m.K)	0.613	18.0
β × 105 (1/K)	21	0.85
dp (nm)	0.384	29

III. GOVERNING EQUATIONS

Governing equations describing the conservation of total mass, momentum, thermal energy, and nanoparticles for the laminar, two-dimensional and steady state natural convection are written as:

$$\nabla.V^* = 0 \tag{1}$$

$$V^*.\nabla V^* = -\frac{1}{\rho_{nf}}\nabla p + \nabla\tau + g \tag{2}$$

$$V^*.\nabla T^* = -\frac{1}{c_{nf}\rho_{nf}}\nabla(k.\nabla T^*) + \frac{c_p\rho_p}{c_{nf}\rho_{nf}}\left(D_B^*\nabla\phi^*\nabla T^* + D_T^*\frac{\nabla T^*\nabla T^*}{T_C^*}\right) \tag{3}$$

$$V^*.\nabla\phi^* = \nabla.\left(D_B^*\nabla\phi^* + D_T^*\frac{\nabla T^*}{T_C^*}\right) \tag{4}$$

Where the stress tensor in Eq. 2 is given as [18]:

$$\tau = \mu_{nf}\left(\nabla V^* + \left(\nabla V^*\right)^t\right) \tag{5}$$

Here, ρ_{nf} is the effective density of the nanofluid, μ_{nf} is the effective dynamic viscosity of the nanofluid, ϕ^* is nanoparticle volume fraction and g is the acceleration due to gravity. The coefficients that appear in Eqs. (3) and (4) are the Brownian diffusion coefficient D_B and the thermophoretic diffusion coefficient D_T as reported in [18] are given by:

$$D_B^* = \frac{k_B T^*}{3\pi\mu_f d_p} \tag{6}$$

$$D_T^* = \left(\frac{\mu_f}{\rho_f}\right)\left(0.26\frac{k_f}{2k_f + k_p}\right)\phi^* \tag{7}$$

Where μ_f is the viscosity of the fluid, d_p is the nanoparticle diameter and k_f and k_p are the thermal conductivity of the fluid and particle materials, respectively. The effective density (ρ_{nf}) and heat capacitance $(\rho C_p)_{nf}$ of the nanofluid are defined as:

$$\rho_{nf} = (1-\phi^*)\rho_f + \phi^*\rho_p \tag{8}$$

$$(\rho c_p)_{nf} = (1-\phi^*)(\rho c_p)_f + \phi^*(\rho c_p)_p \tag{9}$$

Thermal diffusivity of the nanofluids is

$$\alpha_{nf} = \frac{k_{nf}}{(\rho c_p)_{nf}} \tag{10}$$

The effective thermal conductivity of the nanofluid is calculated using an empirical model proposed by Chon et al. [25] as follows:

$$\frac{k_{nf}}{k_f} = 1 + 64.7\times\phi^{0.7460}\left(\frac{d_{bf}}{d_p}\right)^{0.3690}\left(\frac{k_p}{k_{bf}}\right)^{0.7476}\times \mathrm{Pr}^{0.9955}\times \mathrm{Re}^{1.2321} \tag{11}$$

Here Pr_T and Re are defined by:

$$\mathrm{Pr} = \frac{\mu_f}{\rho_f\alpha_f} \tag{12}$$

$$\mathrm{Re} = \frac{\rho_f k_B T}{3\pi\mu_f^2 l_f} \tag{13}$$

where $k_B = 1.3807\times10^{-23}\,J/K$ is the Boltzmann's constant, T is temperature (in °K) and l_f is mean–free path of base fluid molecules (in m) given as 0.17 nm for water [24] .This model considers the Brownian random motion created due to the existence of nanoparticles and also the effect of nanoparticle size and temperature on nanofluids thermal conductivity. The correlation provided is valid for nanoparticle sizes ranging between 11 and 150 nm and for temperature, the associated validity range is 21–71°C. Minsta et al. [26] experimentally showed that Chon et al. model predicts the thermal conductivity of nanofluid accurately up to a volume fraction of 9% for both CuO and Al_2O_3 nanoparticles.

Published By:
Blue Eyes Intelligence Engineering and Sciences Publication (BEIESP)

In the current study, the correlation for dynamic viscosity of CuO–water nanofluid is derived using the available experimental data of Nguyen et al. [27] as a function of temperature and volume fraction of nanoparticles as follows:

$$\mu_{cuo}(cp) = -0.6967 + \frac{15.937}{T} + 1.238\phi + \frac{1356.14}{T^2} - 0.259\phi^2 - 30.88\frac{\phi}{T} - \frac{19652.74}{T^3} + 0.01593\phi^3 + 4.38206\frac{\phi^2}{T} + 147.573\frac{\phi}{T^2} \quad (14)$$

The viscosity in Eq. (14) is expressed in centipoise and the temperature in °C. The R^2 of the regression is 99.8% and a maximum error is 5%.

It is worth noting that the following correlation [28] has been used to evaluating water dynamic viscosity:

$$\mu = A\times 10^{\frac{B}{T-C}},\ C=140,\ B=247,\ A=2.414e-5 \quad (15)$$

Where T is temperature in °K and μ is viscosity in centipoise. The above equations can be converted to non–dimensional form, using the following dimensionless parameters

$$X=\frac{x^*}{L},\quad Y=\frac{y^*}{L},\quad \mathrm{U,V}=\frac{(u,v)L}{\alpha_{f_0}},\quad \mu=\frac{\mu_{nf}}{\mu_{f_0}}$$
$$\theta=\frac{T^*-T_C}{T_H-T_C},\quad F=\frac{\phi^*}{\phi_b},\quad \alpha=\frac{\alpha_{nf}}{\alpha_{f_0}},\quad P=\frac{pL^2}{\rho_{nf}{\alpha_{f_0}}^2} \quad (16)$$
$$D_B=\frac{D_B^*}{D_{B_0}},\quad D_T=\frac{D_T^*}{D_{T_0}},\quad \kappa=\frac{k_{nf}}{k_{f_0}}$$

The governing equations can now be written in dimensionless form as follows

$$\frac{\partial U}{\partial X}+\frac{\partial V}{\partial Y}=0 \quad (17)$$

$$U\frac{\partial U}{\partial X}+V\frac{\partial U}{\partial Y}=\frac{\Pr}{(1-\phi)+\phi\frac{\rho_p}{\rho_f}}\left(\frac{\partial}{\partial X}\left(\mu\frac{\partial U}{\partial X}\right)+\frac{\partial}{\partial Y}\left(\mu\frac{\partial U}{\partial Y}\right)\right) - \frac{\partial P}{\partial X} \quad (18)$$

$$U\frac{\partial V}{\partial X}+V\frac{\partial V}{\partial Y}=\frac{\Pr}{(1-\phi)+\phi\frac{\rho_p}{\rho_f}}\left(\frac{\partial}{\partial X}\left(\mu\frac{\partial V}{\partial X}\right)+\frac{\partial}{\partial Y}\left(\mu\frac{\partial V}{\partial Y}\right)\right) - \frac{\partial P}{\partial Y}+\Pr Ra\theta\left[\frac{1}{\frac{(1-\phi)}{\phi}\frac{\rho_f}{\rho_p}+1}\frac{\beta_p}{\beta_f}+\frac{1}{\frac{\phi}{(1-\phi)}\frac{\rho_f}{\rho_p}+1}\right] \quad (19)$$

$$U\frac{\partial \theta}{\partial X}+V\frac{\partial \theta}{\partial Y}=\left(\frac{\partial}{\partial X}\left(\kappa\frac{\partial \theta}{\partial X}\right)+\frac{\partial}{\partial Y}\left(\kappa\frac{\partial \theta}{\partial Y}\right)\right) \times\frac{1}{(1-\phi)+\phi\left(\frac{(\rho c_p)_p}{(\rho c_p)_f}\right)}+\frac{\Pr Le D_T\xi}{Sc}\left(\left(\frac{\partial \theta}{\partial X}\right)^2+\left(\frac{\partial \theta}{\partial Y}\right)^2\right) \times\frac{\Delta T}{T_c}+\frac{\Pr D_B\phi_b\xi}{Sc}\left(\frac{\partial \theta}{\partial X}\frac{\partial F}{\partial X}+\frac{\partial F}{\partial Y}\frac{\partial \theta}{\partial Y}\right) \quad (20)$$

$$U\frac{\partial F}{\partial X}+V\frac{\partial F}{\partial Y}=\frac{\Pr D_B}{Sc}\left(\frac{\partial^2 F}{\partial X^2}+\frac{\partial^2 F}{\partial Y^2}\right) +\frac{\Pr Le D_T}{Sc}\frac{\Delta T}{\phi_b T_c}\left(\frac{\partial^2 \theta}{\partial X^2}+\frac{\partial^2 \theta}{\partial Y^2}\right) \quad (21)$$

Where

$$Ra=\frac{\beta g(T_H-T_C)L^3}{\nu_{f_0}\alpha_{f_0}},\quad \xi=\frac{\rho_p c_p}{(\phi)(\rho c_p)_p+(1-\phi)(\rho c_p)_f}$$
$$Le=\frac{D_{T_0}}{D_{B_0}},\quad \Pr=\frac{\nu_{f_0}}{\alpha_{f_0}},\quad Sc=\frac{\nu_{f_0}}{D_{B_0}} \quad (22)$$

Where the subscript "o" stands for the reference temperature which is taken as 22°C in the present work, whereas the temperature difference between the hot and cold walls is kept constant at 1°C. The dimensionless boundary conditions are as follows

$$U=V=0 \quad at \quad X=0,1 \quad ,Y=0,1$$
$$\theta(0,Y)=1 \quad , \quad \theta(1,Y)=0$$
$$\frac{\partial\theta(X,0)}{\partial Y}=\frac{\partial\theta(X,1)}{\partial Y}=0 \quad (23)$$
$$\frac{\partial F(X,0)}{\partial Y}=\frac{\partial F(X,1)}{\partial Y}=0$$

For relative nanoparticle volumetric fraction (F), the zero particles flux on the boundaries used as reported in [24] is given by

$$\frac{\partial^2\phi}{\partial y^2}=-\frac{1}{N_{BT}}\frac{D_T}{D_B}\left(\frac{\partial^2\theta}{\partial y^2}\right) \quad (24)$$

Where

$$N_{BT}=\frac{T_C D_{B_0}\phi_b}{D_{T_0}\Delta T} \quad (25)$$

Is the ratio of Brownian diffusivity to thermophoretic diffusivity. This type of boundary conditions used for F is more realistic physically in comparison with the F–constant boundary conditions available in most of numerical simulations reported in literature [29, 30].

The heat transfer rate along the left wall is expressed in terms of the local and average Nusselt's numbers Nu and Nu_{avg}, respectively. The local Nusselt number can be expressed as:

$$\mathrm{Nu}=\frac{hH}{k_f} \quad (26)$$

Where the heat transfer coefficient is

$$h=\frac{q}{T_h-T_c} \quad (27)$$

Where q is total heat flux per unit area. In addition to conduction heat flux there is another heat flux as nanoparticle diffusion heat flux, so the total nanofluid energy flux could be written as:

$$q=-k_{nf}\nabla T^*+h_p j_p \quad (28)$$

In equation (28), c_p and h_p are the specific heat and enthalpy of the nanoparticle material, respectively. Hence, in order to taking into account both Brownian and thermophoresis effects in heat transfer rates of nanofluids, the local Nusselt number can be defined as [24]:

$$\mathrm{Nu}=-k\frac{\partial\theta}{\partial y}-\frac{D_{T_0}\rho_p c_p}{k_f}\left(N_{BT}D_B\frac{\partial\phi}{\partial y}+D_T\frac{\partial\theta}{\partial y}\right) \quad (29)$$

Where

$$k=\frac{k_{nf}}{k_{f_0}} \quad (30)$$

Published By:
Blue Eyes Intelligence Engineering
and Sciences Publication (BEIESP)

The first term on the right–hand side of Eq. (26) is the heat flux due to conduction and the second term is the heat flux due to nanoparticle diffusion.

The average Nusselt number is obtained by integrating the above local Nusselt number over the hot vertical wall

$$Nu_{avg} = \int_0^1 Nu(y)\, dy \tag{31}$$

To evaluate Eq. (31), a 1/3 Simpson's rule of integration is implemented.

IV. NUMERICAL PROCEDURE

The dimensionless governing equations were discretized by the dimensional finite volume method. The grid layout was arranged by utilizing collocated grid procedure, while the Hybrid and Quick scheme were adopted for the convection–diffusion terms for calculation in the fluid domain. The coupling between velocity and pressure is solved using the SIMPLEC algorithm [30, 31] and the Rhie and Chow interpolation [32] is used to avoid the checker–board solutions for the pressure.

For these simulations, the convergence was considered to be reached when the relative error on the value of a property per unit mass denoted by Φ between two successive iterations, n and n+1 was smaller than a chosen tolerance:

$$\frac{\sum\left|\Phi_{i,j}^{n+1} - \Phi_{i,j}^{n}\right|}{\sum\left|\Phi_{i,j}^{n+1}\right|} \le 10^{-6} \tag{33}$$

To test and assess grid independence of the solution scheme, the average Nusselt number for seven different grid sizes is performed as shown in Table. 2 in case Ra= 10^5 and ϕ=5%. Based on the results illustrated in the table and considering the accuracy of the results required and computational time involved, an 51×51 uniform grid is used for all of the subsequent numerical calculations.

TABLE II. Grid Independence Study

Grid size	Nu_{avg}
20×20	3.28702
30×30	3.26587
40×40	3.25015
50×50	3.24556
60×60	3.24398
70×70	3.24283

V. CODE VALIDATION

The present FORTRAN code is validated by comparing the present code results against the numerical simulation of Khanafer et al. [15] and Oztab et al. [22] for enclosures filled with a water–Cu nanofluid (Ra = 10^5, ϕ =5%, Pr = 6.2) a shown in Fig. 2. The agreement is found to be good and little differences could be duo to different models that used for nanofluids modeling.

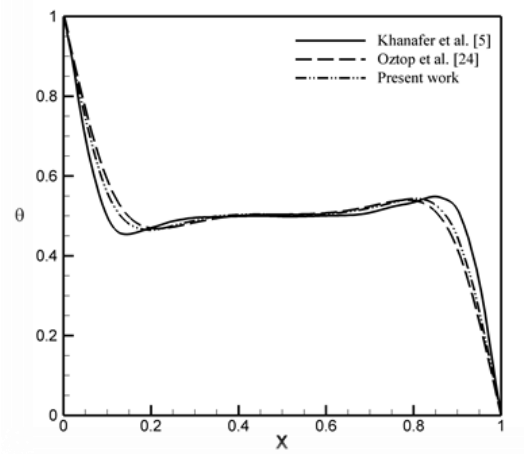

Fig. 2. Validation of the present code against other studies [5, 24] for a square enclosure filled with a Cu-water nanofluid (Ra = 10^5, ϕ =5%, Pr = 6.2)

VI. RESULTS

The overall objective of this current study is to investigate the nanoparticles distribution and heat transfer behavior of natural convection inside a cavity filled with CuO–water nanofluid in both presence and absence of Brownian and thermophoresis effects. The ranges of the magnitude of the Rayleigh numbers and volume fractions of nanoparticles used in this study are Ra=10^4–10^5 and $0 \le \phi \le$ 7%, respectively. It is worth mentioning that the difference between the hot and the cold walls is fixed to 1°C and it is assumed that the Prandtl number (Pr) equals 6.2.

A comparison of the isotherms contours between pure water and the CuO–water nanofluid is conducted for two different values of the Rayleigh number and in the range of $1\% \le \phi \le$ 7% as shown in Fig. 3 (a)–(d). The field of isotherms indicates that these are mostly parallel to the heated and cooled boundaries and vertical to the isolated walls of enclosure. Furthermore, these figures clearly show temperature patterns are influenced by the presence of nanoparticles. That is to say, for low volume fractions (ϕ = 1%), the isotherms are almost identical for both nanofluids and water. Whereas, increasing the nanoparticle concentration for both Rayleigh number, increases deviations of nanofluid and pure water isotherms, especially at the central zone of the enclosure.

Likewise, Fig. 3 illustrates that the thickness of thermal boundary layer next to the heated wall is influenced by the addition of nanoparticles. So that, addition of nanoparticles to the base fluid increases thermal conductivity of the nanofluid and higher values of thermal conductivity are accompanied by higher values of thermal diffusivity.

Published By:
Blue Eyes Intelligence Engineering
and Sciences Publication (BEIESP)

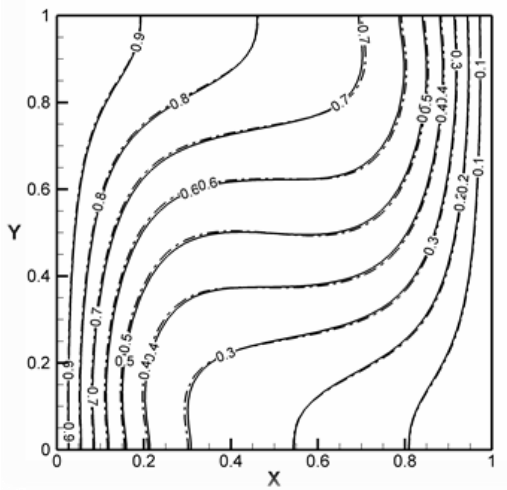

Fig. 3 a. Isotherms of CuO-nanofluid (--) with ϕ = 0.01 and pure water (—) at Ra = 10^4

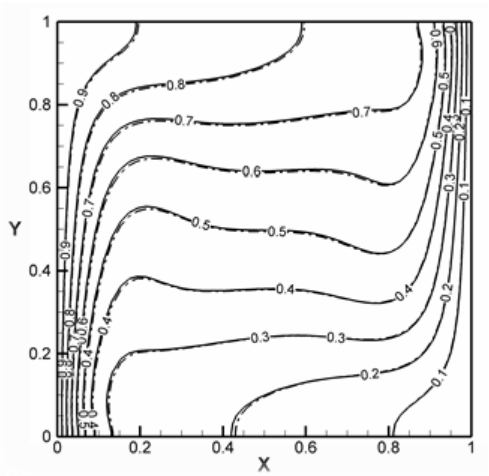

Fig. 3 b. Isotherms of CuO-nanofluid (--) with ϕ = 0.01 and pure water (—) at Ra = 10^5

The high value of thermal diffusivity increases the boundary thickness and this increase in thermal boundary layer thickness has opposite effects on the Nusselt number (according to Eq. (26)). For higher Rayleigh numbers, natural convection become more vigorous and the fluid moves faster and the isotherms become more packed beside adiabatic walls as shown in Fig. 3 (a)–(d).

Variation of local Nusselt number when Brownian and thermophoresis effects are neglected or considered is presented in Fig. 4 (a)–(d) for Ra=10^4 and Ra=10^5. Looking at Fig. 4, it is observed that the heat transfer, by considering the role of Brownian and thermophoresis effects, is higher than the case without considering the role of thermophoresis and Brownian motion for both Rayleigh numbers.

It is worth noting that the heat transfer of nanofluid, by considering the role of Brownian and thermophoresis effects, almost for all values of nanoparticle volume fraction is higher than the pure fluid. However, increasing nanoparticle volume fraction has an adverse effect on heat transfer of CuO–water nanofluid. Whereas, an increase in Nusselt number is observed by increasing the Rayleigh numbers.

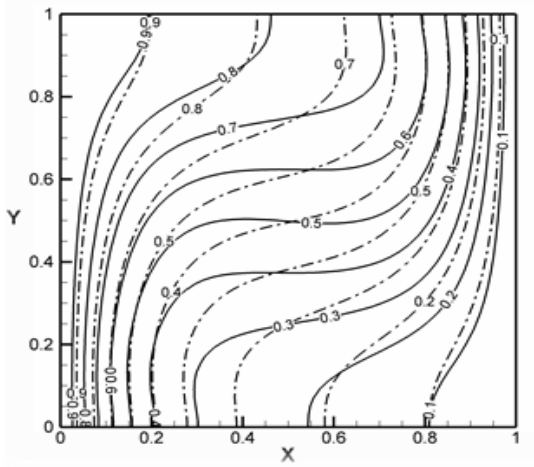

Fig. 3 c. Isotherms of CuO-nanofluid (--) with ϕ = 0.07 and pure water (—) at Ra = 10^4

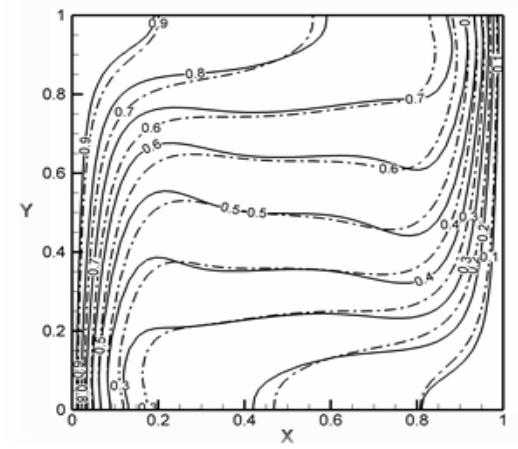

Fig. 3 d. Isotherms of CuO-nanofluid (--) with ϕ = 0.07 and pure water (—) at Ra = 10^5

VII. CONCLUSION

Buoyancy induced flow and heat transfer in a square enclosure filled with a water–Cu nanofluid has been numerically investigated. Main efforts of this investigation were focused on influence of Brownian and thermophoresis effects on the fluid flow and heat transfer characteristics. The following conclusions are drawn. For all values of the solid volume fraction, the heat transfer of water–CuO nanofluid in the presence of Brownian and thermophoresis effects is higher than the pure fluids and it is increased by increasing the Rayleigh. Furthermore, a comparison between the two cases of with and without Brownian and thermophoresis effects shows that higher heat transfer is formed when Brownian motion and thermophoresis effects are considered and there is always a reduction in heat transfer with an increase of the solid volume fraction of the nanofluid.

Published By:
Blue Eyes Intelligence Engineering
and Sciences Publication (BEIESP)

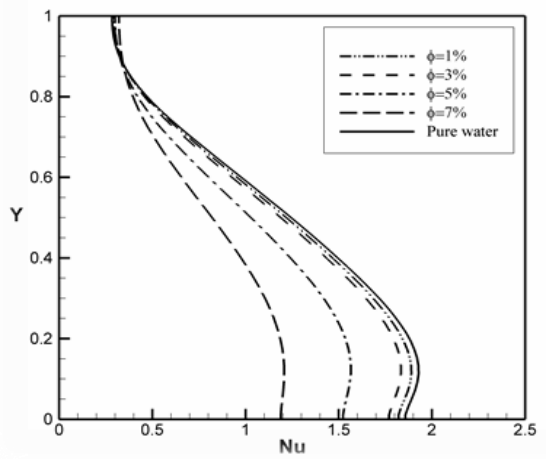

Fig. 4 a. Variation of local Nusselt number along the hot wall for different nanoparticle fractions at Ra=10^4 in the absence of Thermophoresis and Brownian effects

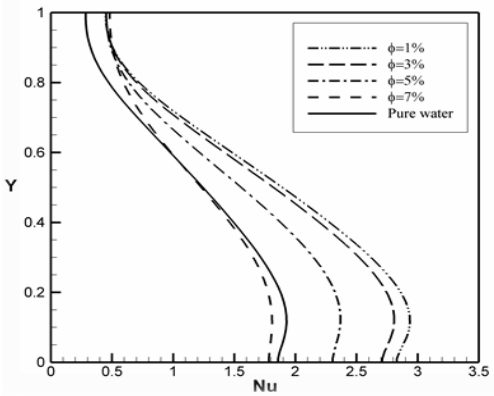

Fig. 4 b. Variation of local Nusselt number along the hot wall for different nanoparticle fractions at Ra=10^4 in the presence of Thermophoresis and Brownian effects

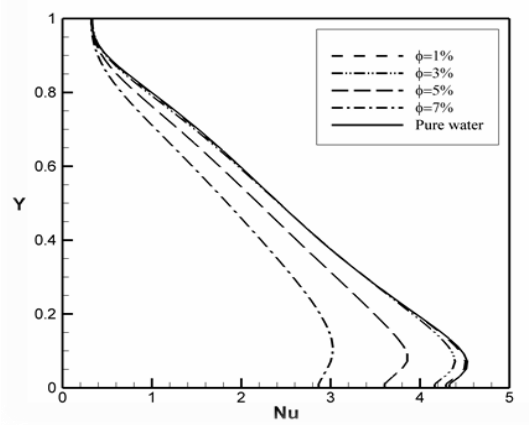

Fig. 4 c. Variation of local Nusselt number along the hot wall for different nanoparticle fractions at Ra=10^5 in the absence of Thermophoresis and Brownian effects

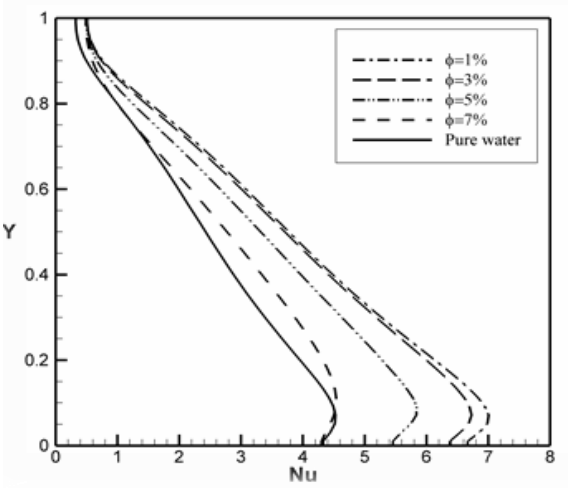

Fig. 4 d. Variation of local Nusselt number along the hot wall for different nanoparticle fractions at Ra=10^5 in the presence of Thermophoresis and Brownian effects

REFERENCES

[1] G.D.VahlDavis, "Natural convection of air in a square cavity, a benchmark numerical solution," *Internat. J. Numr. Methods Fluids* vol. 3, pp. 249–264, 1962

[2] T. Fusegi, J. M. Hyun, K. Kuwahara, B. Farouk, "A numerical study of three dimensional natural convection in a differentially heated cubical enclosure," Int. J. Heat MassTransfer vol. 34, pp. 1543–1557, 1991

[3] G. Barakos, E. Mitsoulis, "Natural convection flow in a square cavity revisited: laminar and turbulent models with wall functions," *Internat. J. Numer. Methods Fluids* Vol. 18, pp. 695–719, 1994

[4] Md. Jashim Uddin, W. A. Khan, and A. I. Md. Ismail, "Review Article Scaling Group Transformation for MHD Boundary Layer Slip Flow of a Nanofluid over a Convectively Heated Stretching Sheet with Heat Generation," *Mathematical Problems in Engineering*, Volume 2012, doi:10.1155/2012/934964

[5] K. Khanafer, K. Vafai, and M. Lightstone, "Buoyancy driven heat transfer enhancement in a two-dimensional enclosure utilizing nanofluids," *International Journal of Heat and Mass Transfer*, vol. 46, no. 19, pp. 3639–3653, 2003.

[6] E. Abu–Nada, Z. Masoud, A. Hijazi, "Natural convection heat transfer enhancement in horizontal concentric annuli using nanofluids," *International Communications in Heat and Mass transfer*, vol. 35, no. 5, pp. 657– 665, 2008.

[7] M. Shahi, A.H. Mahmoudi, A.H. Raouf, "Entropy generation due to natural convection cooling of a nanofluid," *International Communications in Heat and Mass Transfer*, vol. 38, no. 7, pp. 972–983, 2011.

[8] S.M. Aminossadati, B. Ghasemi, "Natural convection of water – CuO nanofluid in a cavity with two pairs of heat source –sink," *International Communications in Heat and Mass Transfer*, vol. 38, pp. 672 –678, 2011

[9] Z.T. Yu, W. Wang, X. Xu, L.W. Fan, Y.C. Hu, K.F. Cen, "A numerical investigation of transient natural convection heat transfer of aqueous nanofluids in a differentially heated square cavity, *International Communications in Heat and Mass transfer*," vol. 38, no. 5, pp. 585–589, 2011.

[10] H.F. Oztop, E. Abu–Nada, "Numerical study of natural convection in partially heated rectangular enclosure filled with nanofluids," *Int. J. Heat Fluid Flow*, Vol. 29, pp. 1326–1336, 2008.

[11] E. Abunada, Z. Masoud, H. F. Oztop, A. Campo, "Effect of nanofluid variable properties on natural convection in enclosures," *International Journal of Thermal Sciences*, vol. 49, No. 3, pp. 479-491, 2010.

[12] F. Lai, Y. Yang, "Lattice Boltzmann simulation of natural convection heat transfer of Al2O3/water nanofluids in a square enclosure," *International Journal of Thermal Sciences*, vol. 50, pp. 1930–1941, 2011

Published By:
Blue Eyes Intelligence Engineering and Sciences Publication (BEIESP)

[13] M. C. Kim, J. S. Hong, C. K. Choi, "The analysis of the onset of Soret–driven convection in nanoparticles suspension," *AIChE Journal*, vol. 52, pp. 2333–2339, 2006.
[14] J. A. Weaver, R. Viskanta, "Natural convection due to horizontal temperature and concentration gradients – 2. Species interdiffusion, Soret and Dufour effects," *International Journal of Heat and Mass Transfer*, vol. 34, pp. 3121–3133, 1991.
[15] Cheng, C. Y., "Soret and Dufour effects on heat and mass transfer by natural convection from a vertical truncated cone in a fluid–saturated porous medium with variable wall temperature and concentration," *Inter. Comm. Heat Mass Transf*., vol. 37, pp. 1031–1035, 2010.
[16] Mustafa, M., Hayat, T., Pop, I., "Stagnation point flow of a nanofluid towards a stretching sheet," *Int. J. Heat and Mass Transfer*, vol. 54, pp. 5588–5594, 2011.
[17] Pal, D., Mondal, H., "Effects of Soret Dufour, chemical reaction and thermal radiation on MHD non–Darcy unsteady mixed convective heat and mass transfer over a stretching sheet," *Comm. Nonlinear Sci. Numer. Sim.*, vol. 16, pp. 1942–1958, 2011.
[18] J. Buongiorno, "Convective transport in nanofluids," *J. Heat Transfer*, vol. 128, pp. 240–250, 2006.
[19] A.V. Kuznetsov, D.A. Nield, "Natural convective boundary layer flow of a nanofluid past a vertical plate," *Int. J. Therm. Sci*., vol. 49, pp. 243–247, 2010.
[20] P. Cheng, W.J. Minkowycz, "Free convection about a vertical fl at plate embedded in a porous medium with application to heat transfer from a dike," *J. Geophys. Res.*, vol. 82, pp. 2040–2044, 1977.
[21] D.A. Nield, A.V. Kuznetsov, "The Cheng–Minkowycz problem for natural convective boundary layer flow in a porous medium saturated by a nanofluid," *Int. J. Heat Mass Transfer*, vol. 52, pp. 5792–5795, 2009.
[22] W.A. Khan, I. Pop, "Boundary layer flow of a nanofluid past a stretching sheet," *Int. J. Heat Mass Transfer*, vol. 53, pp. 2477–2483, 2010.
[23] O.D. Makinde, A. Aziz, "Boundary layer flow of a nanofluid past a stretching sheet with a convective boundary condition," *Int. J. Therm. Sci*., vol. 50, pp. 1326–1332, 2011.
[24] Z. Haddad, E. Abu–Nada, F. Oztop, A. Mataoui, "Natural convection in nanofluids: Are the thermophoresis and Brownian motion effects significant in nanofluid heat transfer enhancement?," *International Journal of Thermal Sciences*, Vol. 57, pp. 152–162, 2012.
[25] C.H. Chon, K.D. Kihm, S.P. Lee, S.U.S. Choi, "Empirical correlation finding the role of temperature and particle size for nanofluid (Al2O3) thermal conductivity enhancement," *Appl. Phys. Lett.*, Vol. 87, no. 15, pp. 153–157, 2005.
[26] H. Angue Minsta, G. Roy, C.T. Nguyen, D. Doucet, "New temperature and conductivity data for water–based nanofluids," *Int. J. Therm . Sci*., vol. 48, no. 2, pp. 363–373, 2008.
[27] C.T. Nguyen, F. Desgranges, G. Roy, N. Galanis, T. Mare, S. Boucher, H. Angue Minsta, "Temperature and particle size dependent viscosity data for water based nanofluids– hysteresis phenomenon," *Int. J. Heat Fluid Flow*, vol. 28 , pp. 1492–1506, 2007.
[28] K.D. Hagen, *Heat Transfer with Applications*, pp. 637–638, Prentice–Hall, New Jersey, USA, 1999.
[29] A. Aziz, W.A . Khan, "Natural convective boundary layer flow of a nanofluid past a convectively heated vertical plate," *International Journal of Thermal Sciences*, vol. 52, pp. 83–90, 2012.
[30] N. Bachok, A. Ishak , I. Pop, "Unsteady boundary–layer flow and heat transfer of a nanofluid over a permeable stretching/shrinking sheet," *International Journal of Heat and Mass Transfer*., Vol. 55, pp. 2102–2109, 2012.
[31] Versteeg, H. K., Malalasekera, W., *an Introduction to Computational Fluid Dynamics. The finite Volume Method*, Longman, London, 1995.
[32] Patankar, S. V., *Numerical heat transfer and fluid flow*, New York: McGraw–Hill, 1980.
[33] Rhie, C. M., Chow, W. L., "Numerical study of the turbulent flow past an airfoil with trailing edge separation," *J. of Heat and Fluid Flow*, Vol. 16, pp. 11–15, 1995.
[34] E.B. Ogut, "Natural convection of water–based nanofluids in an inclined enclosure with a heat source," *International Journal of Thermal Sciences*, vol. 48, no. 11, pp. 2063 –2073, 2009.
[35] E. Abu–Nada, "Rayleigh–Bénard convection in nanofluids: effect of temperature dependent properties," *Int. J. Therm. Sci.*, vol. 50, pp. 1720–1730, 2011.